Journal of Computational Applied Mechanics 2022, 53 (4) 599-625
DOI: 10.22059/jcamech.2022.350620.768

RESEARCH PAPER

Generalized Integral Transform Method for the Bending Analysis of Clamped Rectangular Thin Plates

Charles Chinwuba Ike*

Department of Civil Engineering Enugu State University of Science and Technology, Agbani 402004 Enugu State, Nigeria

Abstract

The article presents Generalized Integral Transform Method (GITM) for the bending analysis of clamped rectangular thin plates. The problem is a boundary value problem (BVP) represented by a fourth order partial differential equation (PDE). Linear combinations of product of eigenfunctions of vibrating clamped thin beams in the in-plane dimensions are used to formulate the sought for deflection function $w(x, y)$ in terms of a double series with unknown generalized deflection parameters c_{mn}. The GITM converts the BVP to an integral equation and ultimately to an algebraic problem in terms of c_{mn}, which is solved to fully obtain $w(x, y)$ as a double infinite series found to be convergent. Bending moments are obtained using the bending moment deflection relations as double infinite series with convergent properties. The solutions obtained for deflection and bending moments at the center and middle of the clamped edges for the two considered cases of uniformly distributed load and hydrostatic load are in agreement with previous results in literature. The effectiveness of the GITM for the clamped plate problem is thus illustrated.

Keywords: Generalized Integral Transform Method, boundary value problem, Kirchhoff plate theory, bending moments, integral equation, eigenfunction.

1. Introduction

Plates are three-dimensional (3D) structural members which may be subjected to transverse static or dynamic, and/or inplane compressive forces. Plates may be homogeneous or nonhomogeneous; composite, laminated, functionally graded, linear elastic or nonlinear in their material properties. They may occur in various geometrical shapes such as rectangular, polygonal, circular, elliptical, oval. They may be considered depending on the loading as dynamic, stability or static elasticity problems. They are classified as thin, moderately thick and thick depending on the ratio of the transverse dimension to the smaller inplane dimension. For thin plate, which is considered in this study the ratio of the thickness to the least inplane dimension is less than 0.05.

Simplifying assumptions have reduced the 3D nature of the general plate problem to two-dimensional (2D) idealizations, and the classical thin plate theory is a 2D simplification of the 3D plate theory. The extensive use of plates in all the major fields of engineering has provoked interest in their studies.

* Corresponding author. Tel.: +2348033101883.
E-mail address: charles.ike@esut.edu.ng

Kirchhoff's plate theory (KPT) assumed the following: [1-20]

- normality (orthogonality) of cross-sectional planes to the middle surface prior to bending deformation and after bending deformation.
- The thickness does not change during bending deformation.

The advantages of the KPT are:

- the resulting domain equation of equilibrium is linear.
- the domain equation contains only one unknown function – transverse deflection $w(x, y)$.
- Bending moments and shear force expressions can be found from the transverse deflection.
- the KPT gives parabolic variation of shear stresses τ_{yz} and τ_{zx} over the thickness in agreement with structural mechanics.

The disadvantage are the limitation to small deformations, and the inability to account for transverse shear deformations, thus limiting the applicability to thin plates where transverse shear deformations are insignificant [18, 21].

Nwoji et al [6] presented flexural solutions for simply supported rectangular Mindlin plates under bisinusoidal load.

Shimpi and Patel [22] derived a two variable refined plate theory for orthotropic plate analysis. Ghugal and Gajbhiye [23] presented flexural solutions of thick isotropic plates using fifth order shear deformation theory which accounted for transverse shear deformations. Ghugal and Sayyad [24] used trigonometric shear deformation theory to solve bending problems of thick isotropic plates. Sayyad and Ghugal [23] presented an exponential shear deformation theory for thick isotropic plates.

Numerical methods such as finite difference method (FDM), finite element method (FEM), differential quadrature method (DQM), discrete singular convolution method (DSCM) have been used to solve the bending problems of plates with different boundary conditions, loading distributions and material types.

However those numerical methods in general yield approximate solutions though with acceptable errors if finer meshes are used and this is the main demerit of the method.

Closed form solutions to plate flexure problems are relatively rare due to the mathematical/analytical rigour involved in finding solutions that apply at all points on the domain including the boundaries.

The classical semi-inverse methods used by Navier and Levy are applicable only to rectangular plates with two opposite simply supported edges.

Superposition method which can be used for solving elastostatic plate bending problems with various boundary conditions, involves complicated solution process.

Symplectic elasticity method for plate problems have been developed by Cui [25], Ma [26], Lim et al [27, 28], Zhong and Li [29] and Wang et al [26].

The symplectic elasticity method demands rigorous analytical manipulations which require highly skilled researchers in mathematical physics.

It is very difficult to obtain solutions to the bending problems of plates with free edges [30, 31].

Aginam et al [32] used the direct variational method (DVM) to solve isotropic rectangular Kirchhoff plate problems under uniform loading and different boundary conditions. Onyeka and Mama [33] and Onyeka et al [34] have similarly studied bending of thin plates using DVM. Onyeka et al [57] have applied the DVM to solve buckling problems of thick plates.

Mbakogu and Pavlović [35] presented variational symbolic solutions to the bending of clamped orthotropic rectangular plates. Evans [36] and Young [37] presented flexural solutions of clamped rectangular plates.

Khan et al [38] applied variational iteration methods to rectangular clamped plate problems.

Sadiq et al [39] used the differential transform method (DTM) to study the nonlinear vibration of functionally graded circular plates resting on two-parameters foundation. Sadiq et al [40] have also used a mathematical procedure to study the natural vibration characteristics of Kirchhoff plate inside fluid medium, resting on one- and two-parameter foundations.

Recently, Salawu et al [41, 42] have investigated the vibration characteristics of circular plates resting on Winkler and Pasternak foundations. The forced vibration solutions of circular plates supported on nonlinear viscoelastic foundation have been presented by Salawu et al [43].

Qian et al [30] derived closed form bending solutions to rectangular thin plate problems with different boundary conditions using the two-dimensional generalized finite integral transformation method (GFITM).

They found that the transformation reduced the governing partial differential equations of the plate to an easily solvable algebraic problem. The merit of the procedure is the avoidance of apriori assumptions of the deflection basis function. Qian et al [31] used 2D GITM to obtain bending solutions of thin plates. Qian et al [30] used the finite integral transform method for the flexural analysis of orthotropic rectangular thin plates with two adjacent edges free and the others clamped or simply supported. Oguaghamba and Ike [2] used the single finite Fourier sine transform method for the eigenfrequency analysis of thin plates. Nwoji et al [8] applied Ritz variational method to obtain accurate bending solutions of rectangular thin plate under hydrostatic load. Ike [9] used Galerkin-Vlasov method to find flexural solutions of rectangular thin plate on Winkler foundation. Onyia et al [3] applied Galerkin-Kantorovich method to obtain accurate elastic buckling solutions of rectangular SCSC plates. Onyia et al [4] applied Galerkin-Vlasov method for the elastic stability analysis of SSCF and SSSS rectangular plates.

Akbas [44-46] has solved complicated non-linear problems of plates using several variants of differential quadrature (DQ) methods. DQ methods have proved to be powerful numerical tools for PDEs. DQMs are easy to use and straightforward in implementation. However, similar to conventional point discretization methods like collections and FDMs, DQMs encounter difficulties for differential equations with singular functions like the Dirac-delta function. This arises due to difficulties introduced by the singularity to the discretization of the problem field.

Yinksel and Akbas [47-50] have also presented the buckling, bending and free vibrations solutions of complex plate problems using DQMs and other numerical techniques. Other scholarly contributions to the theory of elasticity and applications to beams, plates and nanoplates could be found in references [51-95].

1.1 Main Practical Applications of the Study

The main practical applications of the thin plate bending problem studied in thin paper is in the analysis and design of reinforced concrete slabs with rectangular shapes and clamped boundaries where the slab is subjected to uniformly distributed transverse loads and/or hydrostatic loads.

1.2 Differences between this Study and Previous Studies in the Literature

The major difference between this study and previous studies in the literature is that for the first time to the author’s knowledge, a rigorous, first principles application of the GITM is applied to the bending problem of thin rectangular plates with clamped boundaries and where the plate is subjected to uniformly distributed loading and where the plate is subjected to hydrostatic loads.

1.3 Advantages of the Generalized Integral Transform Method

(i) It makes it possible to obtain solution to various BVP and Initial Value Problems (IVPs) for parabolic PDPs in semi-analytical form.
(ii) It reduces the corresponding PDE problems to the Volterva integral equation (VIE) of the second kind.
(iii) Many classes of problems are difficult to solve, or algebraically unwieldy in their original presentations but could be mapped into another domain in which manipulating and solving the equation becomes easier than in the original domain. the solution is then found in the original domain by mapping back from the transform domain back to the original domain with the inverse of the integral transform.
(iv) In the GITM the kernel functions are the eigenfunctions of a freely vibrating thin beam with equivalent restraints conditions as the plate in the x and y coordinate directions; and since these eigenfunctions are constructed to satisfy the boundary conditions at the edges of the plate.
(v) Integral transforms are important tools for solving differential and integral equations because of the simplifications that they bring about, in converting the problems to simpler algebraic problems to simpler algebraic problems, and because they take automatic account of the boundary conditions.

1.4 Disadvantages of GITM

The main disadvantage of the GITM is in the rigorous integration problems involved when dealing with complicated loading and boundary conditions. Another disadvantage is that complicated contour integration problems sometimes need to be solved in order to obtain inversion of the transformed problem back to the physical domain of the original problem.

Literature shows that few mathematically rigourous methods based on the Generalized Integral Transform Methodology have been used for the bending problems of fully clamped Kirchhofff plates. This paper presents the bending analysis of CCCC Kirchhoff plate from a mathematically rigourous perspective using GITM. The bending problem, governed by a fourth order PDE is rigourously presented using the GITM as an integral equation which further reduced to an algebraic problem; effectively offering some simplification to the original problem since the coordinate functions are determined apriori as the eigenfunctions of vibrating thin beams with fixed ends.

2. Theoretical Framework

The theoretical framework for the classical Kirchhoff thin plate theory is adopted in this study for modelling the plate. The governing equations are constructed by simultaneously considering Kinematics, constitutive relations and the differential equation of equilibrium [1].

The linear strain displacement equations of the KPT are

$$\varepsilon_{xx} = \frac{\partial u}{\partial x} \qquad \gamma_{xy} = \frac{\partial v}{\partial x} + \frac{\partial u}{\partial y}$$
$$\varepsilon_{yy} = \frac{\partial v}{\partial y} \qquad \gamma_{zx} = \frac{\partial u}{\partial z} + \frac{\partial w}{\partial x} \tag{1}$$
$$\varepsilon_{zz} = \frac{\partial w}{\partial z} \qquad \gamma_{yz} = \frac{\partial w}{\partial y} + \frac{\partial v}{\partial z}$$

where u, v and w are the displacement components in x, y and z coordinate directions respectively ε_{xx}, ε_{yy}, ε_{zz} are normal strains in the x, y and z directions γ_{xy}, γ_{yz}, γ_{zx} are shear strains.

Kirchhoff-Love hypothesis state that the normals to the middle plate surface are straight and unstructured, and this implies that the shear strain the z direction γ_{xz} are negligible.

Hence from $\gamma_{yz} = \gamma_{xz} = 0$ (2)

$$\frac{\partial v}{\partial z} \simeq -\frac{\partial w}{\partial y}$$
$$\frac{\partial u}{\partial z} \simeq -\frac{\partial w}{\partial x}$$

Hence, $u(x, y, z)$, $v(x, y, z)$ can be explicitly stated as:

$$u = u_0 + z\frac{\partial u_0}{\partial z} + 0(2) \simeq u_0 - z\frac{\partial w_0}{\partial x}$$
$$v = v_0 + z\frac{\partial v_0}{\partial z} + 0(2) \simeq v_0 - z\frac{\partial w_0}{\partial y} \tag{3}$$

The kinematics equations then become:

$$\varepsilon_{xx} = \varepsilon_x^0 + zk_x$$
$$\varepsilon_{yy} = \varepsilon_y^0 + zk_y \tag{4}$$
$$\gamma_{xy} = \gamma_{xy}^0 + 2zk_{xy}$$

where k_x, k_y and k_{xy} are curvatures of the middle plane and ε_x^0, ε_y^0 and γ_{xy}^0 are the strains of the middle plane, given by

$$\varepsilon_x^0 = \frac{\partial u_0}{\partial x}$$
$$\varepsilon_y^0 = \frac{\partial v_0}{\partial y} \tag{5}$$

$$\gamma_{xy}^0 = \frac{\partial v_0}{\partial x} + \frac{\partial u_0}{\partial y}$$

For zero in-plane consultants, all strains at the middle plane are zero, and the kinematics equations are

$$\varepsilon_x = zk_x = -z\frac{\partial^2 w_0}{\partial x^2}$$

$$\varepsilon_y = zk_y = -z\frac{\partial^2 w_0}{\partial y^2}$$

$$\gamma_{xy} = 2zk_{xy} = -2z\frac{\partial^2 w_0}{\partial x \partial y} \tag{6}$$

2.1 Stress – Strain Equations

General form of the stress-strain equations is

$$\sigma = [E_1]\varepsilon = -z[E_1]k \tag{7}$$

where E_1 is the elasticity matrix.

The bending and twisting moments are

$$M = \begin{pmatrix} M_{xx} \\ M_{yy} \\ M_{xy} \end{pmatrix} = \int_{-h/2}^{h/2} -\sigma z\, dz = \int_{-h/2}^{h/2} E_1 z^2\, dz\, k = Dk \tag{8}$$

$$D = \frac{Eh^3}{12(1-\mu^2)} \tag{8a}$$

2.2 Strain Energy

The strain energy integral $U(w)$ is expressed in terms of displacement as:

$$U(w) = \frac{1}{2}\iiint_V \sigma^T \varepsilon\, dV = \frac{1}{2}\iiint \varepsilon^T E_1 \varepsilon\, dV = \frac{1}{2}\iint_A \int_{-h/2}^{b/2} z^2 k^T E_1 k\, dz\, A$$

$$= \frac{1}{2}\iint_A k(w)^T Dk(w)\, dA = \frac{1}{2}\iint M^T k(w)\, dA \tag{9}$$

For isotropic homogeneous plates,

$$U(w)\frac{1}{2}D\iint_{R^2}\left[\left(\frac{\partial^2 w}{\partial x^2}\right)^2 + 2\mu\frac{\partial^2 w}{\partial x^2}\frac{\partial^2 w}{\partial y^2} + \left(\frac{\partial^2 w}{\partial y^2}\right)^2 + 2(1-\mu)\left(\frac{\partial^2 w}{\partial x \partial y}\right)^2\right]dxdy \tag{10}$$

For transversely applied loads, the load potential function is

$$W(w) = -\iiint_V F^T u\, dV = -\iint_{R^2} p(x,y)w\, dxdy \tag{11}$$

Differential Equation of Equilibrium

The general form of the total potential energy functional, Π is:

$$\prod = U + W = \iiint_V F(x, y, w, w_x, w_{xx}, w_{xy}, w_{yy})\, dV \tag{12}$$

The differential equation of equilibrium is obtained using the Euler-Lagrange equations

$$\frac{\partial F}{\partial w} - \frac{\partial}{\partial x}\frac{\partial F}{\partial w,_x} - \frac{\partial}{\partial y}\frac{\partial F}{\partial w,_y} + \frac{\partial^2}{\partial x^2}\frac{\partial F}{\partial w,_{xx}} + \frac{\partial^2}{\partial x \partial y}\frac{\partial F}{\partial w,_{xy}} + \frac{\partial^2}{\partial y^2}\frac{\partial F}{\partial w,_{yy}} = 0 \tag{13}$$

For isotropic homogeneous plates the Euler-Lagrange differential equation is

$$-p + \frac{D}{2}\left[\frac{\partial^2}{\partial x^2}(2w,_{xx} + 2\mu w,_{yy}) + \frac{\partial^2}{\partial x \partial y}(4(1-\mu)w,_{xy} + \frac{\partial^2}{\partial y^2}(2w,_{yy} + 2\mu w,_{xx})\right] = 0 \tag{14}$$

$$-p+\frac{D}{2}\left(2\frac{\partial^4 w}{\partial x^4}+2\mu\frac{\partial^4 w}{\partial x^2\partial y^2}+4(1-\mu)\frac{\partial^4 w}{\partial x^2\partial y^2}+2\frac{\partial^4 w}{\partial y^4}+2\mu\frac{\partial^4 w}{\partial x^2\partial y^2}\right)=0 \tag{15}$$

Hence,

$$\frac{\partial^4 w(x,y)}{\partial x^4}+2\frac{\partial^4 w(x,y)}{\partial x^2\partial y^2}+\frac{\partial^4 w(x,y)}{\partial y^4}=\frac{p}{D} \tag{16}$$

Kirchhoff thin plate theory is adopted. The governing equation is given by the fourth order non-homogeneous partial differential equation

$$D\nabla^2\nabla^2 w(x,y)=p(x,y) \tag{16a}$$

where $D=\dfrac{Eh^3}{12(1-\mu^2)}$

D is the modulus of flexural rigidity of the plate, $w(x,y)$ is the transverse deflection, $p(x,y)$ is the transverse load distribution, x, y are the in-plane Cartesian coordinates. h is the plate thickness, μ is the Poisson's ratio of the plate material. E is the Young's modulus of elasticity. ∇^2 is the Laplace operator, and $\nabla^2\nabla^2 = \nabla^4$ is the biharmonic operator.

The origin of the coordinates is chosen at a corner of the plate and the plate domain is then defined by: $0\le x\le a,\quad 0\le y\le b,$

where a and b are the in-plane dimensions (length and width) of the plate. The xy plane coincides with the middle surface and thus:

$$-\frac{h}{2}\le z\le\frac{h}{2}$$

The bending moments (M_{xx}, M_{yy}) and twisting moment (M_{xy}) distributions are expressed as:

$$M_{xx}=-D\left(\frac{\partial^2 w}{\partial x^2}+\mu\frac{\partial^2 w}{\partial y^2}\right) \tag{17a}$$

$$M_{yy}=-D\left(\frac{\partial^2 w}{\partial y^2}+\mu\frac{\partial^2 w}{\partial x^2}\right) \tag{17b}$$

$$M_{xy}=M_{yx}=-D(1-\mu)\frac{\partial^2 w}{\partial x\partial y} \tag{17c}$$

The shear force distribution (Q_x, Q_y) are:

$$\begin{aligned}Q_x&=-D\frac{\partial}{\partial x}(\nabla^2 w)=-D\frac{\partial}{\partial x}\left(\frac{\partial^2 w}{\partial x^2}+\frac{\partial^2 w}{\partial y^2}\right)\\ Q_y&=-D\frac{\partial}{\partial y}(\nabla^2 w)=-D\frac{\partial}{\partial y}\left(\frac{\partial^2 w}{\partial x^2}+\frac{\partial^2 w}{\partial y^2}\right)\end{aligned} \tag{18}$$

The effective shear forces V_x, V_y are:

$$\begin{aligned}V_x&=-D\frac{\partial}{\partial x}\left(\frac{\partial^2 w}{\partial x^2}+(2-\mu)\frac{\partial^2 w}{\partial y^2}\right)\\ V_y&=-D\frac{\partial}{\partial y}\left(\frac{\partial^2 w}{\partial y^2}+(2-\mu)\frac{\partial^2 w}{\partial x^2}\right)\end{aligned} \tag{19}$$

For fully clamped plates at the edges $x=0,\quad x=a,\quad y=0,\quad y=b,$ the boundary conditions on the deflections are:

$$\begin{aligned}&w(x=0,y)=w(x=a,y)=0\\ &\frac{\partial w}{\partial x}(x=0,y)=\frac{\partial w}{\partial x}(x=a,y)=0\\ &w(x,y=0)=w(x,y=b)=0\end{aligned} \tag{20}$$

$$\frac{\partial w}{\partial y}(x, y=0) = \frac{\partial w}{\partial y}(x, y=b) = 0$$

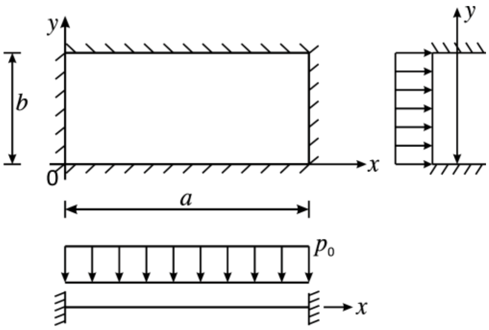

Figure 1: Clamped plate subjected to uniformly distributed load intensity p_0

3. Methodology

3.1 Basis Functions

The Generalized Integral Transform Method employs the eigenfunctions of freely vibrating beams of equivalent span and support conditions as the basis functions. Thus the basis functions in the *x*-coordinate direction is:

$$F_m(x) = (\cosh\beta_m x - \cos\beta_m x) - \lambda_m(\sinh\beta_m x - \sin\beta_m x) \tag{21}$$
$$0 \le x \le a, \quad m = 1, 2, 3, \ldots$$

where $\lambda_m = \dfrac{\sinh\beta_m a + \sin\beta_m a}{\cosh\beta_m a - \cos\beta_m a}$ (22)

and β_m is the m^{th} root of the transcendental equation:

$$\cosh\beta_m a \cos\beta_m a = 1 \tag{23}$$

Similarly, the basis function in the *y* coordinate direction is:

$$G_n(y) = (\cosh\beta_n y - \cos\beta_n y) - \lambda_n(\sinh\beta_n y - \sin\beta_n y) \tag{24}$$
$$0 \le y \le b, \quad n = 1, 2, 3, \ldots$$

where $\lambda_n = \dfrac{\sinh\beta_n b + \sin\beta_n b}{\cosh\beta_n b - \cos\beta_n b}$ (25)

and β_n is the *n*th root of the transcendental equation:

$$\cosh\beta_n b \cos\beta_n b = 1 \tag{26}$$

The roots of the transcendental equation are found using computational software tools as:

$$\begin{aligned} &m = 1, \beta_1 a = 4.73004 \\ &m = 2, \beta_2 a = 7.85321 \\ &m = 3, \beta_3 a = 10.9956 \\ &m = 4, \beta_4 a = 14.13717 \\ &m = 5, \beta_5 a = 17.27876 \\ &m > 5, \beta_m a \simeq \pi\left(\tfrac{1}{2} + m\right) \end{aligned} \tag{27}$$

Similarly,

$$\begin{aligned} &n = 1, \beta_1 b = 4.73004 \\ &n = 2, \beta_2 b = 7.85321 \\ &n = 3, \beta_3 b = 10.9956 \\ &n = 4, \beta_4 b = 14.13717 \\ &n = 5, \beta_5 b = 17.27876 \end{aligned} \tag{28}$$

$n = 5, \beta_n b \simeq \pi\left(\frac{1}{2} + n\right)$

Then $w(x, y)$ is the double infinite series of basis functions in the *x* and *y* coordinate directions:

$$w(x, y) = \sum_{m=1}^{\infty}\sum_{n=1}^{\infty} c_{mn} F_m(x) G_n(y) \tag{29}$$

in which c_{mn} is the generalized deflection parameter which we seek to obtain such that the double series satisfies the governing equation over the plate domain.

It is verifiable that $F_m(x)$ and $G_n(y)$ satisfy the boundary conditions of deflection at the clamped boundaries. Thus

$$\begin{aligned} &F_m(x = 0) = F_m(x = a) = 0 \\ &F'_m(x = 0) = F'_m(x = a) = 0 \\ &G_n(y = 0) = G_n(y = b) = 0 \\ &G'_n(y = 0) = G'_n(y = b) = 0 \end{aligned} \tag{30}$$

where the primes denote space derivatives.

3.2 Generalized Integral Transformation of the Governing Equation

The generalized integral transformation of the governing equation is the integral equation (IE):

$$\int_0^a\int_0^b \left(\nabla^4 \sum_{m=1}^{\infty}\sum_{n=1}^{\infty} c_{mn} F_m(x) G_n(y) - \frac{p_0(x, y)}{D}\right) F_{\bar{m}}(x)(G_{\bar{n}}(y))dxdy = 0 \tag{31}$$

Here, the integral kernel $k(x, y)$ is:

$$k(x, y) = F_{\bar{m}}(x) G_{\bar{m}}(y) \tag{32}$$

$$k(x, y) = \{(\cosh\beta_{\bar{m}}x - \cos\beta_{\bar{m}}x) - \lambda_m(\sinh\beta_{\bar{m}}x - \sin\beta_{\bar{n}}x)\}\{(\cosh\beta_{\bar{n}}y - \cos\beta_{\bar{n}}y) - \lambda_n(\sinh\beta_{\bar{n}}y - \sin\beta_{\bar{n}}y)\} \tag{33}$$

Simplifying,

$$\sum_{m=1}^{\infty}\sum_{n=1}^{\infty} c_{mn} \int_0^a\int_0^b (\nabla^4 F_m(x) G_n(y)) F_{\bar{m}}(x) G_{\bar{n}}(y) dxdy = \frac{1}{D}\int_0^a\int_0^b p(x, y) F_{\bar{m}}(x) G_{\bar{n}}(x) dxdy$$

$$= \frac{1}{D}\int_0^a\int_0^b m = 1\sum_{m=1}^{\infty}\sum_{n=1}^{\infty} p_{mn} F_m(x) G(y) F_{\bar{m}} G_{\bar{n}}\ dxdy \tag{34}$$

The basis functions are orthogonal functions and hence we have:

$$\sum_{m=1}^{\infty}\sum_{n=1}^{\infty} c_{mn} \int_0^a\int_0^b (\nabla^4 F_m(x) G_n(y)) F_m(x) G_n(y) dxdy = \frac{1}{D}\sum_{m=1}^{\infty}\sum_{n=1}^{\infty}\int_0^a\int_0^b p_{mn} F_m^2(x) G_n^2(x) dxdy \tag{35}$$

Further simplification gives:

$$\sum_{m=1}^{\infty}\sum_{n=1}^{\infty} c_{mn} \int_0^a\int_0^b (F_m^{iv}(x) G_n(y) + 2F''_m(x) G''_n(y) + F_m(x) G_n^{iv}(y)) F_m(x) G_n(y) dxdy = \frac{1}{D}\sum_{m=1}^{\infty}\sum_{n=1}^{\infty}\int_0^a\int_0^b p_{mn} F_m^2(x) G_n^2(x) dxdy$$

…(36)

Thus,

$$\sum_{m=1}^{\infty}\sum_{n=1}^{\infty} c_{mn} \int_0^a\int_0^b (F_m^{iv}(x) F_m(x) G_n^2(y) + 2F_m(x) F''_m(x) G''_n(y) G_n(y) + F_m^2(x) G_n^{iv}(y) G_n(y)) dxdy$$

$$= \frac{1}{D}\sum_{m=1}^{\infty}\sum_{n=1}^{\infty}\int_0^a\int_0^b p_{mn} F_m^2(x) G_n^2(y) dxdy = \frac{I_{mn}}{D} \tag{37}$$

$$I_{mn} = \int_0^a\int_0^b p(x, y) F_m(x) G_n(y) dxdy = \int_0^a\int_0^b p_{mn} F_m^2(x) G_n(x) dxdy = \frac{I_{mn}}{D} \tag{38}$$

Generalized integral transformation of the load, function gives:

$$p(x,y)=\sum_{m=1}^{\infty}\sum_{n=1}^{\infty}p_{mn}F_m(x)G_n(y) \tag{38a}$$

$$I_{mn}=\sum_{m=1}^{\infty}\sum_{n=1}^{\infty}\int_0^a\int_0^b p_{mn}F_m^2(x)G_n^2(y)\,dxdy \tag{38b}$$

where p_{mn} is the GITM coefficients of the load distribution.
p_{mn} is found as:

$$p_{mn}=\frac{\int_0^a\int_0^b p(x,y)F_m(x)G_n(y)\,dxdy}{\int_0^a\int_0^b F_m^2(x)G_n^2(y)\,dxdy} \tag{38c}$$

We consider three cases of load distributions

$$p(x,y)=p_0 \tag{39a}$$

$$p(x,y)=p_1(x) \tag{39b}$$

$$p(x,y)=p_2(y) \tag{39c}$$

Then for $p(x,y)=p_0$

$$\int_0^a\int_0^b p(x,y)F_m(x)G_n(y)dxdy=p_0\int_0^a F_m(x)dx\int_0^b G_n(y)dy=p_0I_{1m}I_{2n} \tag{40}$$

where $I_{1m}=\int_0^a F_m(x)dx$ (41)

$$I_{2n}=\int_0^b G_n(y)dy \tag{42}$$

Alternatively for $p(x,y)=p_0$,

$$p_{mn}=\frac{\int_0^a\int_0^b p_0F_m(x)G_n(y)\,dxdy}{\int_0^a\int_0^b F_m^2(x)G_n^2(y)\,dxdy} \tag{43a}$$

$$p_{mn}=\frac{p_0\int_0^a F_m(x)\,dx\int_0^b G_n(y)\,dy}{\int_0^a F_m^2(x)\,dx\int_0^b G_n^2(y)\,dy} \tag{43b}$$

$$p_{mn}=\frac{p_0I_{1m}I_{2n}}{I_{9m}I_{6n}} \tag{43c}$$

I_{mn} is then found from Equation (38b).
For $p(x,y)=p_1(x)$

$$\int_0^a\int_0^b p(x,y)F_m(x)G_n(y)dxdy=\int_0^a\int_0^b p_1(x)F_m(x)G_n(y)dxdy=\int_0^a p_1(x)F_n(x)dx\int_0^b G_n(y)dy=I_{3m}I_{2n} \tag{43}$$

$$I_{3m} = \int_0^a p_1(x)F_m(x)\,dx \tag{44}$$

Alternatively for $p(x,y) = p_1(x)$

$$p_{mn} = \frac{\int_0^a\int_0^b p_1(x)F_m(x)G_n(y)\,dxdy}{\int_0^a\int_0^b F_m^2(x)G_n^2(y)\,dxdy} \tag{44a}$$

$$p_{mn} = \frac{\int_0^a p_1(x)F_m(x)\,dx\int_0^b G_n(y)\,dy}{\int_0^a\int_0^b F_m^2(x)G_n^2(y)\,dxdy} \tag{44b}$$

Hence I_{mn} can be found using Equation (38b).

For $p(x,y) = p_2(y)$

$$\int_0^a\int_0^b p(x,y)F_m(x)G_n(y)dxdy = \int_0^a\int_0^b p_2(y)F_m(x)G_n(y)dxdy = \int_0^a F_m(x)dx\int_0^b p_2(y)G_n(y)dy = I_{1m}I_{4n} \tag{45}$$

$$I_{4n} = \int_0^b p_2(y)G_n(y)dy \tag{46}$$

For $p(x,y) = p_2(y)$,

$$p_{mn} = \frac{\int_0^a\int_0^b p_2(y)F_m(x)G_n(y)\,dxdy}{\int_0^a\int_0^b F_m^2(x)G_n^2(y)\,dxdy} \tag{46a}$$

$$p_{mn} = \frac{\int_0^a F_m(x)\,dx\int_0^b p_2(y)G_n(y)\,dy}{\int_0^a F_m^2(x)\,dx\int_0^b G_n^2(y)\,dy} \tag{46b}$$

Let $I_{5m} = \int_0^a F_m^{iv}(x)F_m(x)\,dx$

$$I_{6n} = \int_0^b G_n^2(y)dy$$

$$I_{7m} = \int_0^a F_{2m}''(x)F_m(x)\,dx \tag{47}$$

$$I_{8m} = \int_0^a G_n''(y)G_n(y)\,dy$$

$$I_{9m} = \int_0^a F_m^2(x)dx$$

$$I_{10n} = \int_0^b G_n^{iv}(y)G_n(y)\,dy$$

Then, for $p(x,y) = p_0$,

$$\sum_{m=1}^{\infty}\sum_{n=1}^{\infty} c_{mn}(I_{5m}I_{6n} + 2I_{7m}I_{8n} + I_{9m}I_{10n}) = \frac{p_0}{D} I_{1m}I_{2n} \tag{48}$$

Then

$$c_{mn} = \frac{p_0 I_{1m}I_{2n}}{D(I_{5m}I_{6n} + 2I_{7m}I_{8n} + I_{9m}I_{10n})} \tag{49}$$

Hence in general,

$$\sum_{m=1}^{\infty}\sum_{n=1}^{\infty} C_{mn}(I_{5m}I_{6n} + 2I_{2m}I_{8n} + I_{9m}I_{10n}) = \frac{1}{D}\sum_{m=1}^{\infty}\sum_{n=1}^{\infty} p_{mn}F_m^2(x)G_n^2(y)\,dxdy \tag{49a}$$

For $p(x,y) = p_0$,

$$p_{mn} = \frac{p_0 I_{1m}I_{2n}}{I_{9m}I_{6n}}$$

$$\sum_{m=1}^{\infty}\sum_{n=1}^{\infty} C_{mn}(I_{5m}I_{6n} + 2I_{7m}I_{8n} + I_{9m}I_{10n}) = \frac{1}{D}\sum_{m=1}^{\infty}\sum_{n=1}^{\infty} \frac{p_0 I_m I_{2n}}{I_{9m}I_{6n}} \int_0^a\int_0^b F_m^2(x)G_n^2(y)\,dxdy \tag{49b}$$

For $p(x,y) = p_1(x)$,

$$\sum_{m=1}^{\infty}\sum_{n=1}^{\infty} c_{mn}(I_{5m}I_{6n} + 2I_{7m}I_{8n} + I_{9m}I_{10n}) = I_{3m}I_{2n} \tag{50}$$

$$c_{mn} = \frac{I_{3m}I_{2n}}{D(I_{5m}I_{6n} + 2I_{7m}I_{8n} + I_{9m}I_{10n})} \tag{51}$$

For $p(x,y) = p_2(y)$,

$$\sum_{m=1}^{\infty}\sum_{n=1}^{\infty} c_{mn}(I_{5m}I_{6n} + 2I_{7m}I_{8n} + I_{9m}I_{10n}) = I_{1m}I_{4n} \tag{52}$$

$$c_{mn} = \frac{I_{1m}I_{4n}}{D(I_{5m}I_{6n} + 2I_{7m}I_{8n} + I_{9m}I_{10n})} \tag{53}$$

In general for $p(x,y)$,

$$\sum_{m=1}^{\infty}\sum_{n=1}^{\infty} c_{mn}(I_{5m}I_{6n} + 2I_{7m}I_{8n} + I_{9m}I_{10n}) = \frac{F_{mn}}{D} \tag{54}$$

Then,

$$c_{mn} = \frac{I_{mn}}{D(I_{5m}I_{6n} + 2I_{7m}I_{8n} + I_{9m}I_{10n})} \tag{55}$$

Then,

$$w(x,y) = \sum_{m=1}^{\infty}\sum_{n=1}^{\infty} \frac{I_{mn}F_m(x)G_n(y)}{D(I_{5m}I_{6n} + 2I_{7m}I_{8n} + I_{9m}I_{10n})} \tag{56}$$

Bending moments

By differentiation

$$w_{xx} = \sum_{m=1}^{\infty}\sum_{n=1}^{\infty}\frac{I_{mn}F_m''(x)G_n(y)}{D(I_{5m}I_{6n} + 2I_{7m}I_{8n} + I_{9m}I_{10n})} \tag{57a}$$

$$w_{yy} = \sum_{m=1}^{\infty}\sum_{n=1}^{\infty}\frac{I_{mn}F_m(x)G_n''(y)}{D(I_{5m}I_{6n} + 2I_{7m}I_{8n} + I_{9m}I_{10n})} \tag{57b}$$

Then,

$$M_{xx} = -\sum_{m=1}^{\infty}\sum_{n=1}^{\infty}\frac{I_{mn}(F_m''(x)G_n(y) + \mu F_m(x)G_n''(y))}{(I_{5m}I_{6n} + 2I_{7m}I_{8n} + I_{9m}I_{10n})} \tag{58a}$$

$$M_{yy} = -\sum_{m=1}^{\infty}\sum_{n=1}^{\infty}\frac{I_{mn}(F_m(x)G_n''(y) + \mu F_m''(x)G_n(y))}{(I_{5m}I_{6n} + 2I_{7m}I_{8n} + I_{9m}I_{10n})} \tag{58b}$$

Deflection and Bending Moments at the Plate Center ($x = a/2$, $y = b/2$)

At the plate center, $x = a/2$, $y = b/2$, then the deflection at the plate center is found as the double series expression:

$$w\left(x = \frac{a}{2}, y = \frac{b}{2}\right) = \sum_{m=1}^{\infty}\sum_{n=1}^{\infty}\frac{I_{mn}F_m(a/2)G_n(b/2)}{D(I_{5m}I_{6n} + 2I_{7m}I_{8n} + I_{9m}I_{10n})} \tag{59}$$

The bending moments at the center (M_{xxc}, M_{yyc}) are found as the double series:

$$M_{xxc} = -\sum_{m=1}^{\infty}\sum_{n=1}^{\infty}\frac{I_{mn}(F_m''(a/2)G_n(b/2) + \mu F_m(a/2)G_n''(b/2)}{(I_{5m}I_{6n} + 2I_{7m}I_{8n} + I_{9m}I_{10n})} \tag{60a}$$

$$M_{yyc} = -\sum_{m=1}^{\infty}\sum_{n=1}^{\infty}\frac{I_{mn}(F_m(a/2)G_n''(b/2) + \mu F_m^{n}(a/2)G_n(b/2)}{(I_{5m}I_{6n} + 2I_{7m}I_{8n} + I_{9m}I_{10n})} \tag{60b}$$

Bending moments at $(x = 0,\ y = b/2)$

At the point $x = 0$, $y = b/2$,

$$M_{xx}\left(x = 0, y = \frac{b}{2}\right) = -\sum_{m=1}^{\infty}\sum_{n=1}^{\infty}\frac{I_{mn}(F_m^{n}(0)G_n(b/2) + \mu F_m(0)G_n''(b/2)}{(I_{5m}I_{6n} + 2I_{7m}I_{8n} + I_{9m}I_{10n})} \tag{61}$$

$$M_{yy}\left(x = 0, y = \frac{b}{2}\right) = -\sum_{m=1}^{\infty}\sum_{n=1}^{\infty}\frac{I_{mn}(F_m(0)G_n''(b/2) + \mu F_m''(0)G_n(b/2)}{(I_{5m}I_{6n} + 2I_{7m}I_{8n} + I_{9m}I_{10n})} \tag{62}$$

Bending moment expressions at $x = a$, $y = b/2$

$$M_{xx}\left(x = a, y = \frac{b}{2}\right) = -\sum_{m=1}^{\infty}\sum_{n=1}^{\infty}\frac{I_{mn}(F_m''(a)G_n(b/2) + \mu F_m(a)G_n''(b/2)}{(I_{5m}I_{6n} + 2I_{7m}I_{8n} + I_{9m}I_{10n})} \tag{63}$$

$$M_{yy}\left(x = a, y = \frac{b}{2}\right) = -\sum_{m=1}^{\infty}\sum_{n=1}^{\infty}\frac{I_{mn}(F_m(a)G_n''(b/2) + \mu F_m''(a)G_n(b/2)}{(I_{5m}I_{6n} + 2I_{7m}I_{8n} + I_{9m}I_{10n})} \tag{64}$$

Bending moment expressions at $x = a/2$, $y = 0$

They are:

$$M_{xx}\left(x = \frac{a}{2}, y = 0\right) = -\sum_{m=1}^{\infty}\sum_{n=1}^{\infty}\frac{I_{mn}(F_m''(a/2)G_n(0) + \mu F_m(a/2)G_n''(0)}{(I_{5m}I_{6n} + 2I_{7m}I_{8n} + I_{9m}I_{10n})} \tag{65}$$

$$M_{yy}\left(x = \frac{a}{2}, y = 0\right) = -\sum_{m=1}^{\infty}\sum_{n=1}^{\infty}\frac{I_{mn}(F_m(a/2)G_n''(0) + \mu F_m''(a/2)G_n(0)}{(I_{5m}I_{6n} + 2I_{7m}I_{8n} + I_{9m}I_{10n})} \tag{66}$$

Bending moment expressions at $x = a/2$, $y = b$

$$M_{xx}\left(x = \frac{a}{2}, y = b\right) = -\sum_{m=1}^{\infty}\sum_{n=1}^{\infty}\frac{I_{mn}(F_m''(a/2)G_n(b) + \mu F_m(a/2)G_n''(b)}{(I_{5m}I_{6n} + 2I_{7m}I_{8n} + I_{9m}I_{10n})} \tag{67}$$

$$M_{yy}\left(x=\frac{a}{2}, y=b\right) = -\sum_{m=1}^{\infty}\sum_{n=1}^{\infty}\frac{I_{mn}\,(F_m(a/2)G_n''(b)+\mu F_m''(a/2)G_n(b)}{(I_{5m}I_{6n}+2I_{7m}I_{8n}+I_{9m}I_{10n})} \quad (68)$$

4. Results

By differentiation,

$$F_m'(x)=\beta_m\{(\sinh\beta_m x+\sin\beta_m x)-\lambda_m(\cosh\beta_m x-\cos\beta_m x)\} \quad (69)$$

$$F_m''(x)=\beta_m^2\{(\cosh\beta_m x+\cos\beta_m x)-\lambda_m(\sinh\beta_m x+\sin\beta_m x)\} \quad (70)$$

$$F_m'''(x)=\beta_m^3\{(\sinh\beta_m x-\sin\beta_m x)-\lambda_m(\cosh\beta_m x+\cos\beta_m x)\} \quad (71)$$

$$F_m^{iv}(x)=\beta_m^4\{(\cosh\beta_m x-\cos\beta_m x)-\lambda_m(\sinh\beta_m x-\sin\beta_m x)\}=\beta_m^4 F_m(x) \quad (72)$$

Similarly,

$$G_n''(y)=\beta_n^2\{(\cosh\beta_n y+\cos\beta_n y)-\lambda_n(\sinh\beta_n y+\sin\beta_n y)\} \quad (73)$$

$$G_n^{iv}(y)=\beta_n^4 G_n(y) \quad (74)$$

$$F_m^2(x)=(\cosh\beta_m x-\cos\beta_m x)^2-2\lambda_m(\cosh\beta_m x-\cos\beta_m x)(\sinh\beta_m x-\sin\beta_m x)+\lambda_m^2(\sinh\beta_m x-\sin\beta_m x)^2 \quad (75)$$

$$F_m''(x)F_m(x)=\{(\cosh\beta_m x-\cos\beta_m x)-\lambda_m(\sinh\beta_m x-\sin\beta_m x)\}\{\beta_m^2(\cosh\beta_m x+ \cos\beta_m x)-\lambda_m(\sinh\beta_m x+\sin\beta_m x)\} \quad (76)$$

$$F_m(x)F_m''(x)=\beta_m^2\{(\cosh^2\beta_m x-\cos^2\beta_m x)-\lambda_m(\sinh\beta_m x-\sin\beta_m x)(\cosh\beta_m x+\cos\beta_m x)- \lambda_m(\sinh\beta_m x+\sin\beta_m x)(\cosh\beta_m x-\cos\beta_m x)+\ \lambda_m^2(\sinh^2\beta_m x-\sin^2\beta_m x)\} \quad (77)$$

$$F_m''F_m=\beta_m^2\{(\cosh^2\beta_m x-\cos^2\beta_m x)-\lambda_m(\sinh\beta_m x\cosh\beta_m x-\sin\beta_m x\cosh\beta_m x+ \sinh\beta_m x\cos\beta_m x-\sin\beta_m x\cos\beta_m x+\sinh\beta_m x\cosh\beta_m x+\sin\beta_m x\cosh\beta_m x)+ \lambda_m^2(\sinh^2\beta_m x-\sin^2\beta_m x)\} \quad (78)$$

$$F_m''F_m=\beta_m^2\left\{\cosh^2\beta_m x-\cos^2\beta_m x)+\lambda_m^2(\sinh^2\beta_m x-\sin^2\beta_m x)- \lambda_m(2\sinh\beta_m x\cosh\beta_m x-2\sin\beta_m x\cos\beta_m x)\right\} \quad (79)$$

$$F_m^{iv}(x)F_m(x)=\beta_m^4 F_m^2(x) \quad (80)$$

$$2\cosh\beta_m x\cos\beta_m x+\cos^2\beta_m x \quad (81)$$

$$(\sinh\beta_m x-\sin\beta_m x)^2=\sinh^2\beta_m x+\sin^2\beta_m-2\sinh\beta_m x\sin\beta_m x \quad (82)$$

$$(\cosh\beta_m x-\cos\beta_m x)(\sinh\beta_m x-\sin\beta_m x)=\cosh\beta_m x\sinh\beta_m x-\cos\beta_m x\sinh\beta_m x- \cosh\beta_m x\sin\beta_m x+\cos\beta_m x\sin\beta_m x=\cosh\beta_m x\sinh\beta_m x+\cos\beta_m x\sin\beta_m x- \cos\beta_m x\sinh\beta_m x-\cosh\beta_m x\sin\beta_m x \quad (83)$$

Similarly,

$$G_n''(y)G_n(y)=\beta_n^2\left\{(\cosh^2\beta_n y-\cos^2\beta_n y)+\lambda_n^2(\sinh^2\beta_n y-\sin^2\beta_n y)- \lambda_n(2\sinh\beta_n y\cosh\beta_n y-2\sin\beta_n y\cos\beta_n y)\right\} \quad (84)$$

$$G_n^{iv}(y)G_n(y)=\beta_n^4 G_n^2(y) \quad (85)$$

$$I_{1m}=\int_0^a\{(\cosh\beta_m x-\cos\beta_m x)-\lambda_m(\sinh\beta_m x-\sin\beta_m x)\}dx \quad (86)$$

$$I_{1m}=\left[\left(\frac{\sinh\beta_m x}{\beta_m}-\frac{\sin\beta_m x}{\beta_m}\right)-\lambda_m\left(\frac{\cosh\beta_m x}{\beta_m}+\frac{\cos\beta_m x}{\beta_m}\right)\right]_0^a \quad (87)$$

$$I_{1m}=\left[\left(\frac{\sinh\beta_m a}{\beta_m}-\frac{\sin\beta_m a}{\beta_m}\right)-\lambda_m\left(\frac{\cosh\beta_m a}{\beta_m}+\frac{\cos\beta_m a}{\beta_m}\right)\right]-\left(0-\lambda_m\left(\frac{1}{\beta_m}+\frac{1}{\beta_m}\right)\right) \quad (88)$$

$$I_{1m} = \frac{1}{\beta_m}[(\sinh\beta_m a - \sin\beta_m a) - \lambda_m(\cosh\beta_m a + \cos\beta_m a) + 2\lambda_m] \tag{89}$$

$$I_{2n} = \frac{1}{\beta_n}[(\sinh\beta_n b - \sin\beta_n b) - \lambda_n(\cosh\beta_n b + \cos\beta_n b) + 2\lambda_n] \tag{90}$$

For hydrostatic load distribution,

$$p_1(x) = \frac{q_0 x}{a} \tag{91}$$

where $p_1(x = a) = \frac{q_0 a}{a} = q_0$ and $p_1(x = 0) = 0$

then,

$$I_{mn} = \int_0^a\int_0^b \frac{q_0 x}{a} F_m(x) G_n(y)\, dxdy \tag{92}$$

$$I_{mn} = \frac{q_0}{a}\int_0^a xF_m(x)dx \int_0^b G_n(y)dy \tag{93}$$

$$I_{mn} = \frac{q_0}{a} I_{11m}\, I_{2n} \tag{94}$$

$$I_{11m} = \int_0^a xF_m(x)\, dx \tag{95}$$

With the aid of computational software tools, Wolfram integrator software, Wolfram computational algebra software, MathCad and Mathematica, the deflections are computed at the center of uniformly loaded clamped plates and presented in Table 1. Similarly, the bending moments at the center of uniformly loaded clamped rectangular plates for $\mu = 0.30$ are computed and presented in Table 2. The bending moments at the center of the clamped edges of uniformly loaded rectangular clamped plates are presented in Table 3.

Computational software tools were similarly used to find the deflections and bending moments at the center and middle of the clamped edges of clamped rectangular thin plates under hydrostatic load distribution $p(x, y) = \frac{q_0 x}{a}$. The center deflection for clamped rectangular thin plates under hydrostatic load distribution as determined in the study are shown in Table 4, with comparative results from Timoshenko and Woinowsky-Krieger [96].

Similarly, the bending moment coefficients obtained for clamped rectangular thin plates under hydrostatic load distribution for $\mu = 0.30$ are presented in Table 5 for the center of the plate and Table 6 for the center of the clamped edges.

Table 1: Deflections of rectangular Kirchhoff plate with clamped edges and subjected to uniformly distributed load over the plate domain for $\mu = 0.30$

Aspect ratio (b/a)	$W_c/qa^4/D$ Present study	Imrak and Gerdemeli [45] $W_c/qa^4/D$	Timoshenko and Woinowsky-Krieger [96] and Evans [36] $W_c/qa^4/D$	Taylor and Govindjee [97] $W_c/qa^4/D$
1.0	1.26725×10^{-3}	1.26725×10^{-3}	1.260×10^{-3}	1.26532×10^{-3}
1.1	1.503×10^{-3}		1.50×10^{-3}	
1.2	1.7283×10^{-3}	1.72833×10^{-3}	1.72×10^{-3}	1.72487×10^{-3}
1.3	1.91×10^{-3}		1.91×10^{-3}	
1.4	2.069×10^{-3}	2.07217×10^{-3}	2.07×10^{-3}	2.06814×10^{-3}
1.5	2.203×10^{-3}		2.20×10^{-3}	
1.6	2.303×10^{-3}	2.30399×10^{-3}	2.30×10^{-3}	2.29997×10^{-3}
1.7	2.382×10^{-3}		2.38×10^{-3}	

1.8	2.4499×10^{-3}	2.44989×10^{-3}	2.45×10^{-3}	2.44616×10^{-3}
1.9	2.492×10^{-3}		2.49×10^{-3}	
2	2.536×10^{-3}	2.53625×10^{-3}	2.54×10^{-3}	2.53297×10^{-3}
∞	2.6041×10^{-3}	2.60417×10^{-3}	2.60×10^{-3}	2.60417×10^{-3}

Table 2: Bending moments of the center of rectangular Kirchhoff plate with clamped edges under uniformly distributed load over the plate domain for $(\mu = 0.30)$

Aspect ratio b/a	Present study		Timoshenko and Woinowsky-Krieger [96]	
	M_{xx}/qa^2	M_{yy}/qa^2	M_{xx}/qa^2	M_{yy}/qa^2
1.0	0.0231	0.0231	0.0231	0.0231
1.1	0.0264	0.0231	0.0264	0.0231
1.2	0.0299	0.0288	0.0299	0.0288
1.3	0.0327	0.0222	0.0327	0.0222
1.4	0.0349	0.0212	0.0349	0.0212
1.5	0.0368	0.0203	0.0368	0.0203
1.6	0.0381	0.0193	0.0381	0.0193
1.7	0.0392	0.0182	0.0392	0.0182
1.8	0.0401	0.0174	0.0401	0.0174
1.9	0.0407	0.0165	0.0407	0.0165
2	0.0412	0.0158	0.0412	0.0158
∞	0.0417	0.0125	0.0417	0.0125

Table 3: Bending moments coefficients of the center of the clamped edges of rectangular Kirchhoff plate with clamped edges subjected to uniformly distributed load over the plate domain for $(\mu = 0.30)$

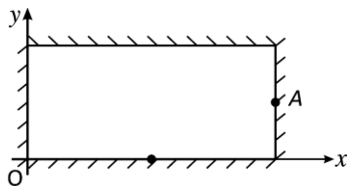

Aspect ratio b/a	Present study		Timoshenko and Woinowsky-Krieger [96]	
	$\frac{M_{xxA}(a,b/2)}{qa^2}$	$\frac{M_{yyA}(a,b/2)}{qa^2}$	M_{xxA}/qa^2	M_{yyA}/qa^2
1.0	–0.0513	–0.0513	–0.0513	–0.0513
1.1	–0.0581	–0.0538	–0.0581	–0.0538
1.2	–0.0639	–0.0554	–0.0639	–0.0554
1.3	–0.0687	–0.0563	–0.0687	–0.0563
1.4	–0.0726	–0.0568	–0.0726	–0.0568
1.5	–0.0757	–0.0570	–0.0757	–0.0570
1.6	–0.0780	–0.0571	–0.0780	–0.0571
1.7	–0.0799	–0.0571	–0.0799	–0.0571
1.8	–0.0812	–0.0571	–0.0812	–0.0571
1.9	–0.0822	–0.0571	–0.0822	–0.0571
2	–0.0829	–0.0571	–0.0829	–0.0571
∞	–0.0833	–0.0571	–0.0833	–0.0571

Table 4: Center deflections of rectangular Kirchhoff plates with clamped edges in case of hydrostatic load distribution over the plate domain for $(\mu = 0.30)$

Aspect ratio (b/a)	Center deflection D/qa^4 Present study	Timoshenko and Woinowsky-Krieger [96] D/qa^4
0.5	0.000080	0.000080
2/3	0.000217	0.000217
1.0	0.00063	0.00063
1.5	0.0110	0.0110
∞	0.0130	0.0130

Table 5: Bending moments at the center of rectangular Kirchhoff plates with clamped edges: case of hydrostatic load distribution over the plate for $(\mu = 0.30)$

Aspect ratio b/a	Present study		Timoshenko and Woinowsky-Krieger [96]	
	M_{xx}/qa^2	M_{yy}/qa^2	M_{xx}/qa^2	M_{yy}/qa^2
0.5	1.98×10^{-3}	5.15×10^{-3}	1.98×10^{-3}	5.15×10^{-3}
2/3	4.51×10^{-3}	8.17×10^{-3}	4.51×10^{-3}	8.17×10^{-3}
1.0	11.5×10^{-3}	11.5×10^{-3}	11.5×10^{-3}	11.5×10^{-3}
1.5	18.4×10^{-3}	10.2×10^{-3}	18.4×10^{-3}	10.2×10^{-3}
∞	20.8×10^{-3}	6.3×10^{-3}	20.8×10^{-3}	6.3×10^{-3}

Table 6: Bending moment coefficients in rectangular Kirchhoff plates with clamped edges: case of hydrostatic load distribution over the plate domain for $(\mu = 0.30)$

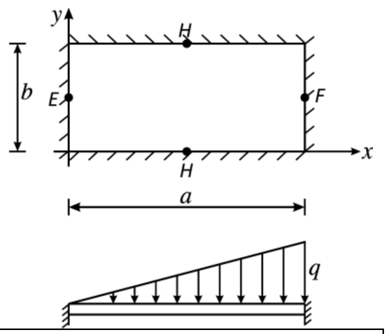

Aspect ratio b/a	Present study			Timoshenko and Woinowsky-Krieger [96]		
	M_{xxE}/qa^2	M_{xxF}/qa^2	M_{yyA}/qa^2	M_{xxE}/qa^2	M_{xxF}/qa^2	M_{yyA}/qa^2
0.5	–0.0028	–0.0115	–0.0104	–0.0028	–0.0115	–0.0104
2/3	–0.0066	–0.0187	–0.0168	–0.0066	–0.0187	–0.0168
1.0	–0.0179	–0.0334	–0.0257	–0.0179	–0.0334	–0.0257
1.5	–0.0295	–0.0462	–0.0285	–0.0295	–0.0462	–0.0285
∞	–0.0333	–0.0500		–0.0333	–0.0500	

5. Discussion

4.1Physical Description of the Studied Problem

The physical descriptions of the studied problem are presented in Figures 2 and 3.

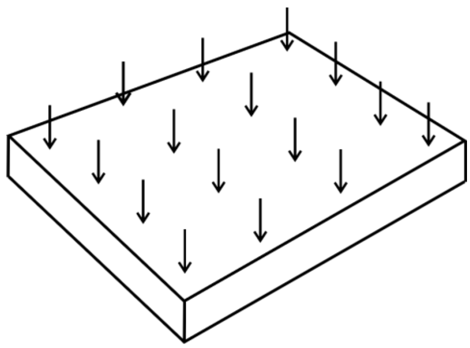

Figure 2: Uniformly loaded thin plate with clamped edges

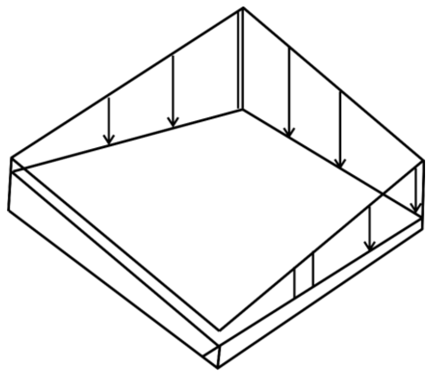

Figure 3: Hydrostatically loaded thin clamped rectangular plate

Figure 2 shows a clamped rectangular Kirchhoff plate which is subjected to a uniformly distributed transverse load of intensity p_0 over the entire plate domain $(0 \geq x \leq a,\ \ 0 \leq y \leq b)$. Figure 3 shows a clamped rectangular Kirchhoff plate which is subjected to a hydrostatic distribution of load over the entire plate domain.

In each case, the plate is considered to be made of homogeneous, isotropic linear elastic material. Such problems are frequently encountered in civil engineering, structural engineering, aeronatutical engineering and naval engineering in the flexural design of rectangular slabs with clamped boundaries.

The Generalized Integral Transform Method (GITM) has been used in this research work to find exact bending solutions to clamped rectangular thin plates under uniform and hydrostatic load distributions.

The GITM employs the eigenfunctions of freely vibrating Euler-Bernoulli beams of equivalent span and boundary conditions as the plate, as the shape functions. For the clamped plate problem studied, the shape functions are given by Equations (11 – 13) for the x coordinate direction, and Equations (14 – 16) for the y coordinate direction.

The unknown deflection $w(x, y)$ is constructed as a double infinite series of $F_m(x)$ and $G_n(y)$ as given in Equation (19) which contains generalized deflection parameters c_{mn}. The deflection thus apriori satisfies all the boundary conditions.

The transformation of the plate problem via the GITM gives the integral equation (IE) given by Equation (31) where the integral kernel is Equation (33). In general, the resulting IE simplifies to a system of algebraic equations given by Equation (37).

Three cases of load variations over the plate domain given by Equations (39a – 39c) were considered. For the case of uniform load, the system of algebraic equations simplified to Equation (48). For load variation in the x direction only, the algebraic equations simplified to Equation (50). For load variation in the y direction only, the algebraic equations simplified to Equation (52). For general load variation in both the x and y directions the algebraic equations simplified to Equation (54).

The unknown parameters c_{mn} are found from the algebraic equations by solving the algebraic problem.

Bending moments M_{xx}, M_{yy} are found from the bending moment-deflection equations. M_{xx} is found in closed form as Equation (58a); a double series expression made of infinite terms. Similarly, M_{yy} is found as the double series expression of infinite terms given by Equation (58b).

Deflection and bending moments were found at the plate center as the double series expressions of infinite terms given respectively by Equations (59), (60a) and (60b).

Bending moment (M_{xx}, M_{yy}) expressions for the middle of clamped edge (at $x = 0$, $y = b/2$) are found as Equations (61) and (62). Bending moment (M_{xx}, M_{yy}) expressions for the middle of clamped edge (at $x = a$, $y = b/2$) are found as Equation (63) and (64). Bending moment expressions for the middle of clamped edge at $x = a/2$, $y = 0$ are found as Equations (65) and (66). Bending moment expressions for the middle of clamped edge at $x = a/2$, $y = b$ are found as Equations (67) and (68).

The specific case of hydrostatic load distribution given by Equation (92) was considered, yielding the integration problem for the load term given by Equation (93). The center deflections of clamped thin plates under uniform load are determined for various plate aspect ratios and shown in Table 1. Table 1 also shows previous results of the problem by Imrak and Gerdemeli [98], Evans [36], Timoshenko and Woinowsky-Krieger [96] and Taylor and Govindjee [89]. Table 1 confirms the agreement of the present GITM solution with previous solutions.

Table 2 displays the center bending moments M_{xx} and M_{yy} (for various aspect ratios of b/a) for clamped plate under uniform load, and confirms the exact solution obtained with the present GITM method and agreement with previous results by Timoshenko and Woinowsky-Krieger [96]. The Bending moments at the center of the clamped edges ($x = a$, $y = b/2$) for various aspect ratios are presented in Table 3 and compared with previous results from Timoshenko and Woinowsky-Krieger [96]. Table 3 confirms the exact solution obtained and the agreement with results by Timoshenko and Woinowsky-Krieger [96].

Table 4 displays the center deflections of clamped plates under hydrostatic load for various aspect ratios and illustrates the exact nature of the present solution and the identity with Timoshenko and Woinowsky-Krieger [96] results. Table 5 shows the bending moments at the center of clamped plate under hydrostatic load and illustrates the exact results obtained and the identity with Timoshenko and Woinowsky-Krieger [96] results.

Table 6 shows the bending moment coefficients at the middle of the clamped edges and illustrates the agreement with Timoshenko and Woinowsky-Krieger [96] results.

6. Conclusion

(i) The unknown deflection function $w(x, y)$ in the BVP of clamped rectangular plate is sought in terms of double infinite series of the linear combinations of products of the two eigenfunctions $F_m(x)$ and $G_n(y)$ of freely vibrating thin beams with clamped ends, where $F_m(x)$ is the eigenfunction of EB beams with clamped ends ($y = 0$, $y = b$); and $G_n(y)$ is the eigenfunction of EB beams with clamped ends ($y = 0$, $y = b$).

(ii) The deflection $w(x, y)$ is expressed in terms of unknown generalized displacement parameters c_{mn} which are determined by requiring that the PDE be satisfied at all points on the domain and on the boundaries.

(iii) The displacement $w(x, y)$ satisfies all the boundary conditions of the CCCC plate since the eigenfunctions $F_m(x)$ and $G_n(y)$ satisfy all the boundary conditions.

(iv) The eigenfunctions $F_m(x)$ and $G_n(y)$ become the integral kernel functions in formulating the BVP as an IE.

(v) The application of the GITM to the governing domain PDE over the domain $(0 \le x \le a, \quad 0 \le y \le b)$ converts it to an integral equation.

(vi) The IE reduces to algebraic problem from which c_{mn} can be found using the methods of linear algebra; and thus yielding the full determination of $w(x, y)$.

(vii) The bending moments M_{xx}, M_{yy} are found using the bending moment deflection equations as double infinite series.

(viii) For the case of CCCC plate under uniform loading, the maximum values of the deflection and bending moments were found to occur at the plate center; and satisfactorily accurate results were obtained using a few terms of the series.

(ix) The expressions for the values of deflection and bending moments at the plate center for uniformly loaded CCCC plates were found to be rapidly convergent.

(x) The GITM yielded closed form analytical expressions for deflection and bending moments for the loading cases of CCCC plate studied. The GITM results for uniform load and for hydrostatic load on CCCC plate were identical with previous results by Timoshenko and Woinowsky-Krieger [96].

Notations/Nomenclature

x, y	in plane Cartesian coordinates
z	transverse Cartesian coordinate
a	in-plane dimension of the plate in the x direction
b	in-plane dimension of the plate in the y direction
h	thickness of the plate
$w(x, y)$	transverse deflection function
$p(x, y)$	transverse load distribution
μ	Poisson's ratio of the plate material
D	modulus of flexural rigidity of the plate
E	Young's modulus of elasticity
3D	three-dimensional
2D	two-dimensional
u, v, w	displacement components in x, y and z coordinate directions respectively
$\varepsilon_{xx}, \varepsilon_{yy}, \varepsilon_{zz}$	normal strains in the x, y, z coordinate directions respectively
$\gamma_{xy}, \gamma_{yz}, \gamma_{xz}$	shear strains
1D	one-dimensional
KPT	Kirchhoff plate theory
IE	Integral Equation
DVM	Direct Variational Method
GFITM	Generalized Finite Integral Transform Method
GITM	Generalized Integral Transform method
FITM	Finite Integral Transform Method
FEM	Finite Element Method
FDM	Finite Difference Method
DQ	Differential Quadrature
DQM	Differential Quadrature Method
DSC	Discrete Singular Convolution
DSCM	Discrete Singular Convolution Method
DTM	Differential Transform Method
M_{xx}, M_{yy}	bending moments
M_{yx}, M_{xy}	twisting moments
Q_x, Q_y	shear force distributions
VIE	Volterra Integral Equation
V_x, V_y	effective shear forces
$F_m(x)$	basis functions in the x coordinate direction
$G_n(y)$	basis functions in the y coordinate direction
$\bar{m}, m, n, \bar{n}$	integers
c_{mn}	generalized deflection parameters
$K(x, y)$	integral kernel function
p_0	integrity of uniformly distributed load
p_{mn}	GITM coefficients of the load distribution function
k_x, k_y, k_{xy}	curvatures of the middle plane of the plate
$\varepsilon_x^0, \varepsilon_y^0, \gamma_{xy}^0$	strains of the middle plane
$[E_1]$	elasticity matrix for plate
k	curvature matrix for plate
ε	strain matrix
σ	stress matrix
M	bending moment matrix
$U(w)$	strain energy functional expressed in terms of transverse displacement, w
$W(w)$	load potential functional expressed in terms of transverse displacement, w
Π	total potential energy functional
$F(x, y, w, w_{,x}, w_{,xx}, w_{,xy}, w_{,yy})$	integrand in the total potential energy functional
V	volume of integration, three-dimensional domain of integrand

A area of integration, two-dimensional domain over which integration is carried out.

Mathematical symbols/notations

∇^2 Laplace operator
∇^4 biharmonic operator
$\geq$ greater than or equal to
$\leq$ less than or equal to
$\frac{\partial}{\partial x}$ partial derivative with respect to *x*
$\frac{\partial}{\partial y}$ partial derivative with respect to *y*
$\frac{\partial^2}{\partial x^2}$ second partial derivative with respect to *x*
$\frac{\partial^2}{\partial y^2}$ second partial derivative with respect to *y*
$\frac{\partial^2}{\partial x \partial y}$ mixed partial derivative with respect to *x* and *y*
cos cosine function
cosh hyperbolic cosine function
sin sine function
sinh hyperbolic sine function
$\int$ single integral
$\iint$ double integral
$\sum\sum$ double summation
$\sum$ summation
∞ infinity
$F_m''(x)$ second derivative of $F_m(x)$ with respect to *x*
$F_m^{iv}(x)$ fourth derivative of $F_m(x)$ with respect to *x*
$G_m''(y)$ second derivative of $G_n(y)$ with respect to *y*
$G_n^{iv}(y)$ fourth derivative of $G_n(y)$ with respect to *y*
w_{xx} second partial derivative of $w(x, y)$ with respect to *x*
w_{yy} second partial derivative of $w(x, y)$ with respect to *y*.

References

[1] C. C. Ike, B. O. Mama, H. N. Onah, C. U. Nwoji, Trefftz displacement potential function method for solving elastic half-space problems, *Civil Engineering and Architecture*, Vol. 9, No. 3, pp. 559-583, 2021.
[2] M. E. Onyia, E. O. Rowland-Lato, C. C. Ike, Elastic buckling analysis of SSCF and SSSS rectangular thin plates using the single finite fourier sine integral transform method, *International Journal of Engineering Research and Technology*, Vol. 13, No. 6, pp. 1147-1158, 2020.
[3] M. E. Onyia, E. O. Rowland-Lato, C. C. Ike, Galerkin-Kantorovich method for the elastic buckling analysis of thin rectangular SCSC plates, *International Journal of Engineering Research and Technology*, Vol. 13, No. 4, pp. 613-619, 2020.

[4] M. E. Onyia, E. O. Rowland-Lato, C. C. Ike, Galerkin-Vlasov variational method for the elastic buckling analysis of SSCF and SSSS rectangular plates, *International Journal of Engineering Research and Technology*, Vol. 13, No. 6, pp. 1137-1146, 2020.

[5] C. C. Ike, B. O. Mama, Kantorovich variational method for the flexural analysis of CSCS Kirchhoff-Love plates, *Mathematical Models in Engineering*, Vol. 4, No. 1, pp. 29-41, 2018.

[6] C. U. Nwoji, B. O. Mama, H. N. Onah, C. C. Ike, Flexural analysis of simply supported rectangular Mindlin plates under bisinusoidal transverse load, *ARPN Journal of Engineering and Applied Sciences*, Vol. 13, No. 15, pp. 4480-4488, 2018.

[7] B. O. Mama, C. C. Ike, C. U. Nwoji, H. N. Onah, Advances in Modelling and Analysis A, *Journal homepage: http://iieta. org/Journals/AMA/AMA_A*, Vol. 55, No. 2, pp. 76-81, 2018.

[8] C. U. Nwoji, H. N. Onah, B. O. Mama, C. C. Ike, M. E. Abd El Hady, A. M. Youssef, A. M. Bayoumy, Y. Z. Elhalwagy, X. Wang, G. Ren, Ritz variational method for bending of rectangular Kirchhoff plate under transverse hydrostatic load distribution, *Mathematical Modelling of Engineering Problems*, Vol. 5, No. 1, pp. 1-10, 2018.

[9] C. Ike, Flexural analysis of rectangular kirchhoff plate on winkler foundation using galerkin-vlasov variational method, *Mathematical Modelling of Engineering Problems*, Vol. 5, No. 2, pp. 83-92, 2018.

[10] C. Nwoji, B. Mama, C. Ike, H. Onah, Galerkin-Vlasov method for the flexural analysis of rectangular Kirchhoff plates with clamped and simply supported edges, *IOSR Journal of Mechanical and Civil Engineering*, Vol. 14, No. 2, pp. 61-74, 2017.

[11] B. Mama, C. Ike, H. Onah, C. Nwoji, Analysis of rectangular Kirchhoff plate on Winkler foundation using finite Fourier sine transform method, *IOSR Journal of Mathematics*, Vol. 13, No. 4, pp. 58-66, 2017.

[12] C. Nwoji, B. Mama, H. Onah, C. Ike, Kantorovich-vlasov method for simply supported rectangular plates under uniformly distributed transverse loads, *methods*, Vol. 14, No. 15, pp. 16, 2017.

[13] B. Mama, C. Nwoji, C. Ike, H. Onah, Analysis of simply supported rectangular Kirchhoff plates by the finite Fourier sine transform method, *International Journal of Advanced Engineering Research and Science*, Vol. 4, No. 3, pp. 237109, 2017.

[14] C. C. Ike, Flexural analysis of Kirchhoff plates on Winkler foundations using finite Fourier sine integral transform method, *Mathematical Modelling of Engineering Problems (MMEP)*, Vol. 4, No. 4, pp. 145-154, 2017.

[15] C. Ike, Kantorovich-Euler lagrange-galerkin's method for bending analysis of thin plates, *Nigerian Journal of Technology*, Vol. 36, No. 2, pp. 351-360, 2017.

[16] B. Mama, H. Onah, C. Ike, N. Osadebe, Solution of free harmonic vibration equation of simply supported Kirchhoff plate by Galerkin-Vlasov method, *Nigerian Journal of Technology*, Vol. 36, No. 2, pp. 361-365, 2017.

[17] C. Ike, C. Nwoji, Kantorovich method for the determination of eigen frequencies of thin rectangular plates, *Exploarematics Journal of Innovative engineering and Technology (EJIET)*, Vol. 1, No. 01, pp. 20-27, 2017.

[18] C. Ike, C. Nwoji, E. Ikwueze, I. Ofondu, Bending analysis of simply supported rectangular Kirchhoff plates under linearly distributed transverse load, *Explorematics Journal of Innovative Engineering and Technology (EJIET)*, Vol. 1, No. 01, pp. 28-36, 2017.

[19] N. Osadebe, C. Ike, H. Onah, C. Nwoji, F. Okafor, Application of the Galerkin-Vlasov method to the Flexural Analysis of simply supported Rectangular Kirchhoff Plates under uniform loads, *Nigerian Journal of Technology,* Vol. 35, No. 4, pp. 732-738, 2016.

[20] C. C. Ikea, Generalized Integral Transform Method for bending and buckling analysis of rectangular thin plate with two opposite edges simply supported and other edges clamped.

[21] G. C. Tsiatas, M. N. Pavlović, Thin rectangular plates under axial point loading: Accuracy of the classical single Fourier series solution for stresses, in *Proceeding of*, Elsevier, pp. 3757-3764.

[22] R. Shimpi, H. Patel, A two variable refined plate theory for orthotropic plate analysis, *International Journal of Solids and Structures,* Vol. 43, No. 22-23, pp. 6783-6799, 2006.

[23] Y. M. Ghugal, P. D. Gajbhiye, Bending analysis of thick isotropic plates by using 5th order shear deformation theory, *Journal of Applied and Computational Mechanics,* Vol. 2, No. 2, pp. 80-95, 2016.

[24] Y. M. Ghugal, A. S. Sayyad, A static flexure of thick isotropic plates using trigonometric shear deformation theory, *Journal of Solid Mechanics,* Vol. 2, No. 1, pp. 79-90, 2010.

[25] C. Shuang, Symplectic elasticity approach for exact bending solutions of rectangular thin plates, *City University of Hong Kong, Hong Kong*, 2007.

[26] B. Wang, P. Li, R. Li, Symplectic superposition method for new analytic buckling solutions of rectangular thin plates, *International Journal of Mechanical Sciences,* Vol. 119, pp. 432-441, 2016.

[27] C. W. Lim, C. Lü, Y. Xiang, W. Yao, On new symplectic elasticity approach for exact free vibration solutions of rectangular Kirchhoff plates, *International Journal of Engineering Science,* Vol. 47, No. 1, pp. 131-140, 2009.

[28] C. W. Lim, S. Cui, W. Yao, On new symplectic elasticity approach for exact bending solutions of rectangular thin plates with two opposite sides simply supported, *International journal of solids and structures,* Vol. 44, No. 16, pp. 5396-5411, 2007.

[29] Y. Zhong, R. Li, Exact bending analysis of fully clamped rectangular thin plates subjected to arbitrary loads by new symplectic approach, *Mechanics Research Communications,* Vol. 36, No. 6, pp. 707-714, 2009.

[30] X. Qian, Z. Jinghui, S. Ullah, Z. Yang, G. Litao, Analytical bending solutions of thin plates by two-dimensional generalized integral transform method, *ZAMM-Journal of Applied Mathematics and Mechanics/Zeitschrift für Angewandte Mathematik und Mechanik,* Vol. 101, No. 6, pp. e202000246, 2021.

[31] Q. Xu, Z. Yang, S. Ullah, Z. Jinghui, Y. Gao, Analytical bending solutions of orthotropic rectangular thin plates with two adjacent edges free and the others clamped or simply supported using finite integral transform method, *Advances in Civil Engineering,* Vol. 2020, 2020.

[32] C. Aginam, C. Chidolue, C. Ezeagu, Application of direct variational method in the analysis of isotropic thin rectangular plates, *ARPN Journal of Engineering and Applied Sciences,* Vol. 7, No. 9, pp. 1128-1138, 2012.

[33] F. Onyeka, B. Mama, Analytical study of bending characteristics of an elastic rectangular plate using direct variational energy approach with trigonometric function, *Emerging Science Journal*, Vol. 5, No. 6, pp. 916-926, 2021.

[34] F. Onyeka, T. Okeke, B. Mama, Static Elastic Bending Analysis of a Three-Dimensional Clamped Thick Rectangular Plate using Energy Method, *HighTech and Innovation Journal,* Vol. 3, No. 3, pp. 267-281, 2022.

[35] F. Mbakogu, M. Pavlović, Bending of clamped orthotropic rectangular plates: a variational symbolic solution, *Computers & Structures,* Vol. 77, No. 2, pp. 117-128, 2000.
[36] T. H. Evans, Tables of moments and deflections for a rectangular plate fixed on all edges and carrying a uniformly distributed load, 1939.
[37] D. Young, Analysis of clamped rectangular plates, 1940.
[38] Y. Khan, P. Tiwari, R. Ali, Application of variational methods to a rectangular clamped plate problem, *Computers & Mathematics with Applications,* Vol. 63, No. 4, pp. 862-869, 2012.
[39] O. Sadiq, M. Sobamowo, S. Salawu, Nonlinear dynamic behaviour of functionally graded circular plates resting on two-parameters foundation using differential transform method, in *Proceeding of,* IOP Publishing, pp. 012114.
[40] O. Sadiq, G. Sobamowo, S. Salawu, Analytical approach to investigation of free vibration of thin rectangular plate immersed in fluid, resting on Winkler and Pasternak foundations, *Karbala International Journal of Modern Science,* Vol. 5, No. 3, pp. 2, 2019.
[41] S. Salawu, G. Sobamowo, O. Sadiq, INVESTIGATION OF THE DYNAMIC BEHAVIOUR OF NON-UNIFORM THICKNESS CIRCULAR PLATES RESTING ON WINKLER AND PASTERNAK FOUNDATIONS, *Acta Polytechnica,* Vol. 60, No. 2, pp. 127-144, 2020.
[42] S. A. Salawu, G. M. Sobamowo, O. M. Sadiq, Forced Vibration Analysis of Isotropic Thin Circular Plate Resting on Nonlinear Viscoelastic Foundation, *Iranian Journal of Science and Technology, Transactions of Civil Engineering,* Vol. 44, No. 1, pp. 277-288, 2020.
[43] S. A. Salawu, G. M. Sobamowo, O. M. Sadiq, Investigation of dynamic behaviour of circular plates resting on Winkler and Pasternak foundations, *SN Applied Sciences,* Vol. 1, No. 12, pp. 1-12, 2019.
[44] Ş. D. AKBAŞ, Stability of a non-homogenous porous plate by using generalized differantial quadrature method, *International Journal of Engineering and Applied Sciences,* Vol. 9, No. 2, pp. 147-155, 2017.
[45] Ş. D. Akbaş, Vibration and static analysis of functionally graded porous plates, *Journal of Applied and Computational Mechanics,* 2017.
[46] Ş. AKBAŞ, Static analysis of a nano plate by using generalized differential quadrature method, *International Journal of Engineering and Applied Sciences,* Vol. 8, No. 2, pp. 30-39, 2016.
[47] Y. Z. YÜKSEL, Ş. D. AKBAŞ, Vibration Analysis of a Sandwich Plate with Laminated Face and Porous Core Layers Resting on Elastic Foundation, *Journal of Innovative Science and Engineering,* Vol. 6, No. 1, pp. 32-45, 2022.
[48] Y. Yuksel, S. Akbas, Hygrothermal stress analysis of laminated composite porous plates, *Structural Engineering and Mechanics,* Vol. 80, No. 1, pp. 1-13, 2021.
[49] Y. Z. Yüksel, Ş. D. Akbaş, Buckling analysis of a fiber reinforced laminated composite plate with porosity, *Journal of Computational Applied Mechanics,* Vol. 50, No. 2, pp. 375-380, 2019.
[50] Y. Z. YÜKSEL, Ş. D. AKBAŞ, Free vibration analysis of a cross-ply laminated plate in thermal environment, *International Journal of Engineering and Applied Sciences,* Vol. 10, No. 3, pp. 176-189, 2018.

[51] M. Mohammadi, A. Farajpour, A. Moradi, M. Hosseini, Vibration analysis of the rotating multilayer piezoelectric Timoshenko nanobeam, *Engineering Analysis with Boundary Elements,* Vol. 145, pp. 117-131, 2022.

[52] M. Mohammadi, A. Rastgoo, Primary and secondary resonance analysis of FG/lipid nanoplate with considering porosity distribution based on a nonlinear elastic medium, *Mechanics of Advanced Materials and Structures,* Vol. 27, No. 20, pp. 1709-1730, 2020.

[53] M. Mohammadi, M. Hosseini, M. Shishesaz, A. Hadi, A. Rastgoo, Primary and secondary resonance analysis of porous functionally graded nanobeam resting on a nonlinear foundation subjected to mechanical and electrical loads, *European Journal of Mechanics-A/Solids,* Vol. 77, pp. 103793, 2019.

[54] M. Mohammadi, A. Rastgoo, Nonlinear vibration analysis of the viscoelastic composite nanoplate with three directionally imperfect porous FG core, *Structural Engineering and Mechanics, An Int'l Journal,* Vol. 69, No. 2, pp. 131-143, 2019.

[55] A. Farajpour, A. Rastgoo, M. Mohammadi, Vibration, buckling and smart control of microtubules using piezoelectric nanoshells under electric voltage in thermal environment, *Physica B: Condensed Matter,* Vol. 509, pp. 100-114, 2017.

[56] A. Farajpour, M. H. Yazdi, A. Rastgoo, M. Loghmani, M. Mohammadi, Nonlocal nonlinear plate model for large amplitude vibration of magneto-electro-elastic nanoplates, *Composite Structures,* Vol. 140, pp. 323-336, 2016.

[57] A. Farajpour, M. Yazdi, A. Rastgoo, M. Mohammadi, A higher-order nonlocal strain gradient plate model for buckling of orthotropic nanoplates in thermal environment, *Acta Mechanica,* Vol. 227, No. 7, pp. 1849-1867, 2016.

[58] M. Mohammadi, M. Safarabadi, A. Rastgoo, A. Farajpour, Hygro-mechanical vibration analysis of a rotating viscoelastic nanobeam embedded in a visco-Pasternak elastic medium and in a nonlinear thermal environment, *Acta Mechanica,* Vol. 227, No. 8, pp. 2207-2232, 2016.

[59] M. R. Farajpour, A. Rastgoo, A. Farajpour, M. Mohammadi, Vibration of piezoelectric nanofilm-based electromechanical sensors via higher-order non-local strain gradient theory, *Micro & Nano Letters,* Vol. 11, No. 6, pp. 302-307, 2016.

[60] M. Baghani, M. Mohammadi, A. Farajpour, Dynamic and stability analysis of the rotating nanobeam in a nonuniform magnetic field considering the surface energy, *International Journal of Applied Mechanics,* Vol. 8, No. 04, pp. 1650048, 2016.

[61] M. Goodarzi, M. Mohammadi, M. Khooran, F. Saadi, Thermo-mechanical vibration analysis of FG circular and annular nanoplate based on the visco-pasternak foundation, *Journal of Solid Mechanics,* Vol. 8, No. 4, pp. 788-805, 2016.

[62] H. Asemi, S. Asemi, A. Farajpour, M. Mohammadi, Nanoscale mass detection based on vibrating piezoelectric ultrathin films under thermo-electro-mechanical loads, *Physica E: Low-dimensional Systems and Nanostructures,* Vol. 68, pp. 112-122, 2015.

[63] M. Safarabadi, M. Mohammadi, A. Farajpour, M. Goodarzi, Effect of surface energy on the vibration analysis of rotating nanobeam, 2015.

[64] M. Goodarzi, M. Mohammadi, A. Gharib, Techno-Economic Analysis of Solar Energy for Cathodic Protection of Oil and Gas Buried Pipelines in Southwestern of Iran, in *Proceeding of,* https://publications.waset.org/abstracts/33008/techno-economic-analysis-of …, pp.

[65] M. Mohammadi, A. A. Nekounam, M. Amiri, The vibration analysis of the composite natural gas pipelines in the nonlinear thermal and humidity environment, in *Proceeding of,* https://civilica.com/doc/540946/, pp.

[66] M. Goodarzi, M. Mohammadi, M. Rezaee, Technical Feasibility Analysis of PV Water Pumping System in Khuzestan Province-Iran, in *Proceeding of*, https://publications.waset.org/abstracts/18930/technical-feasibility …, pp.

[67] M. Mohammadi, A. Farajpour, A. Moradi, M. Ghayour, Shear buckling of orthotropic rectangular graphene sheet embedded in an elastic medium in thermal environment, *Composites Part B: Engineering*, Vol. 56, pp. 629-637, 2014.

[68] M. Mohammadi, A. Moradi, M. Ghayour, A. Farajpour, Exact solution for thermo-mechanical vibration of orthotropic mono-layer graphene sheet embedded in an elastic medium, *Latin American Journal of Solids and Structures,* Vol. 11, pp. 437-458, 2014.

[69] M. Mohammadi, A. Farajpour, M. Goodarzi, F. Dinari, Thermo-mechanical vibration analysis of annular and circular graphene sheet embedded in an elastic medium, *Latin American Journal of Solids and Structures,* Vol. 11, pp. 659-682, 2014.

[70] M. Mohammadi, A. Farajpour, M. Goodarzi, Numerical study of the effect of shear in-plane load on the vibration analysis of graphene sheet embedded in an elastic medium, *Computational Materials Science,* Vol. 82, pp. 510-520, 2014.

[71] A. Farajpour, A. Rastgoo, M. Mohammadi, Surface effects on the mechanical characteristics of microtubule networks in living cells, *Mechanics Research Communications,* Vol. 57, pp. 18-26, 2014.

[72] S. R. Asemi, M. Mohammadi, A. Farajpour, A study on the nonlinear stability of orthotropic single-layered graphene sheet based on nonlocal elasticity theory, *Latin American Journal of Solids and Structures,* Vol. 11, pp. 1541-1546, 2014.

[73] M. Goodarzi, M. Mohammadi, A. Farajpour, M. Khooran, Investigation of the effect of pre-stressed on vibration frequency of rectangular nanoplate based on a visco-Pasternak foundation, 2014.

[74] S. Asemi, A. Farajpour, H. Asemi, M. Mohammadi, Influence of initial stress on the vibration of double-piezoelectric-nanoplate systems with various boundary conditions using DQM, *Physica E: Low-dimensional Systems and Nanostructures,* Vol. 63, pp. 169-179, 2014.

[75] S. Asemi, A. Farajpour, M. Mohammadi, Nonlinear vibration analysis of piezoelectric nanoelectromechanical resonators based on nonlocal elasticity theory, *Composite Structures,* Vol. 116, pp. 703-712, 2014.

[76] M. Mohammadi, M. Ghayour, A. Farajpour, Free transverse vibration analysis of circular and annular graphene sheets with various boundary conditions using the nonlocal continuum plate model, *Composites Part B: Engineering,* Vol. 45, No. 1, pp. 32-42, 2013.

[77] M. Mohammadi, M. Goodarzi, M. Ghayour, A. Farajpour, Influence of in-plane pre-load on the vibration frequency of circular graphene sheet via nonlocal continuum theory, *Composites Part B: Engineering,* Vol. 51, pp. 121-129, 2013.

[78] M. Mohammadi, A. Farajpour, M. Goodarzi, R. Heydarshenas, Levy type solution for nonlocal thermo-mechanical vibration of orthotropic mono-layer graphene sheet embedded in an elastic medium, *Journal of Solid Mechanics,* Vol. 5, No. 2, pp. 116-132, 2013.

[79] M. Mohammadi, A. Farajpour, M. Goodarzi, H. Mohammadi, Temperature Effect on Vibration Analysis of Annular Graphene Sheet Embedded on Visco-Pasternak Foundati, *Journal of Solid Mechanics,* Vol. 5, No. 3, pp. 305-323, 2013.

[80] M. Danesh, A. Farajpour, M. Mohammadi, Axial vibration analysis of a tapered nanorod based on nonlocal elasticity theory and differential quadrature method, *Mechanics Research Communications,* Vol. 39, No. 1, pp. 23-27, 2012.
[81] A. Farajpour, A. Shahidi, M. Mohammadi, M. Mahzoon, Buckling of orthotropic micro/nanoscale plates under linearly varying in-plane load via nonlocal continuum mechanics, *Composite Structures,* Vol. 94, No. 5, pp. 1605-1615, 2012.
[82] M. Mohammadi, M. Goodarzi, M. Ghayour, S. Alivand, Small scale effect on the vibration of orthotropic plates embedded in an elastic medium and under biaxial in-plane pre-load via nonlocal elasticity theory, 2012.
[83] A. Farajpour, M. Mohammadi, A. Shahidi, M. Mahzoon, Axisymmetric buckling of the circular graphene sheets with the nonlocal continuum plate model, *Physica E: Low-dimensional Systems and Nanostructures,* Vol. 43, No. 10, pp. 1820-1825, 2011.
[84] A. Farajpour, M. Danesh, M. Mohammadi, Buckling analysis of variable thickness nanoplates using nonlocal continuum mechanics, *Physica E: Low-dimensional Systems and Nanostructures,* Vol. 44, No. 3, pp. 719-727, 2011.
[85] H. Moosavi, M. Mohammadi, A. Farajpour, S. Shahidi, Vibration analysis of nanorings using nonlocal continuum mechanics and shear deformable ring theory, *Physica E: Low-dimensional Systems and Nanostructures,* Vol. 44, No. 1, pp. 135-140, 2011.
[86] M. Mohammadi, M. Ghayour, A. Farajpour, Analysis of free vibration sector plate based on elastic medium by using new version differential quadrature method, *Journal of solid mechanics in engineering,* Vol. 3, No. 2, pp. 47-56, 2011.
[87] A. Farajpour, M. Mohammadi, M. Ghayour, Shear buckling of rectangular nanoplates embedded in elastic medium based on nonlocal elasticity theory, in *Proceeding of,* www.civilica.com/Paper-ISME19-ISME19_390.html, pp. 390.
[88] M. Mohammadi, A. Farajpour, A. R. Shahidi, Higher order shear deformation theory for the buckling of orthotropic rectangular nanoplates using nonlocal elasticity, in *Proceeding of,* www.civilica.com/Paper-ISME19-ISME19_391.html, pp. 391.
[89] M. Mohammadi, A. Farajpour, A. R. Shahidi, Effects of boundary conditions on the buckling of single-layered graphene sheets based on nonlocal elasticity, in *Proceeding of,* www.civilica.com/Paper-ISME19-ISME19_382.html, pp. 382.
[90] M. Mohammadi, M. Ghayour, A. Farajpour, Using of new version integral differential method to analysis of free vibration orthotropic sector plate based on elastic medium, in *Proceeding of,* www.civilica.com/Paper-ISME19-ISME19_497.html, pp. 497.
[91] N. Ghayour, A. Sedaghat, M. Mohammadi, Wave propagation approach to fluid filled submerged visco-elastic finite cylindrical shells, 2011.
[92] M. Z. Nejad, A. Hadi, A. Omidvari, A. Rastgoo, Bending analysis of bi-directional functionally graded Euler-Bernoulli nano-beams using integral form of Eringen's non-local elasticity theory, *Structural engineering and mechanics: An international journal,* Vol. 67, No. 4, pp. 417-425, 2018.
[93] M. Hosseini, M. Shishesaz, K. N. Tahan, A. Hadi, Stress analysis of rotating nano-disks of variable thickness made of functionally graded materials, *International Journal of Engineering Science,* Vol. 109, pp. 29-53, 2016.
[94] A. Hadi, A. Daneshmehr, S. N. Mehrian, M. Hosseini, F. Ehsani, Elastic analysis of functionally graded Timoshenko beam subjected to transverse loading, *Technical Journal of Engineering and Applied Sciences,* Vol. 3, No. 13, pp. 1246-1254, 2013.

[95] M. Mohammadi, A. Farajpour, A. Rastgoo, Coriolis effects on the thermo-mechanical vibration analysis of the rotating multilayer piezoelectric nanobeam, *Acta Mechanica*, https://doi.org/10.1007/s00707-022-03430-0, 2023.

[96] S. Timoshenko, S. Woinowsky-Krieger, 1959, *Theory of plates and shells*, McGraw-hill New York,

[97] R. L. Taylor, S. Govindjee, Solution of clamped rectangular plate problems, *Communications in numerical methods in engineering*, Vol. 20, No. 10, pp. 757-765, 2004.

[98] C. E. Imrak, I. Gerdemeli, The problem of isotropic rectangular plate with four clamped edges, *Sadhana*, Vol. 32, No. 3, pp. 181-186, 2007.